

Robustness of Enhanced STAR to Multipath Power Profile Variations in Wideband CDMA Channels*

Karim CHEIKHROUHO¹, Sofiène AFFES², and Paul MERMELSTEIN²

1: École Nationale d'Ingénieurs de Tunis

BP 37, Le Belvédère, Tunis, 1002, Tunisia

2: INRS-Télécommunications, Université du Québec

800, de la Gauchetière Ouest, Suite 6900, Montreal, Quebec, H5A 1K6, Canada

{cheikhro,affes,mermel}@inrs-telecom.uquebec.ca

Abstract— We recently proposed an enhanced version [1] of original STAR [2], the spatio-temporal array receiver, and assessed the robustness of its multipath tracking module to various design parameters (*e.g.*, sensitivity to the rolloff factor selection and to pulse-shape errors of raised-cosine shaping filters). Here, we address another dimension that deserves investigation, *i.e.*, the robustness of the tracking module of STAR to possible multipath power profile variations of Rayleigh fading. Link- and system-level simulations suggest that profiles of (0, -3, -6) dB, (0, -6, -10) dB and (0, -10, -10) dB perform nearly as well as the (0, 0, 0) dB reference profile. The maximum capacity loss does not exceed 7% and suggests a strong robustness of STAR to multipath power profile variations. For voice-rate links with low mobility, STAR maintains its performance advantage over the 2D-RAKE by about 50 to 60% in capacity under different radio-propagation conditions.

I. INTRODUCTION

Enhancements in receiver operation for cellular CDMA systems, *e.g.*, signal combining, power control or channel coding, have led to increases in cell capacity and spectrum efficiency and are now included in proposed standards for third generation wireless systems [3]. However, such high-capacity operation requires synchronization at significantly reduced SNR levels.

In a recent work [1], we proposed an enhanced version of STAR, the spatio-temporal array-receiver [2]. Evaluations of uplink capacity for improved STAR and the 2D-RAKE [4] with both perfect and active synchronization indicated that synchronization with early-late gate component of a RAKE-type receiver may constitute a bottleneck to performance improvement. Results also suggest that STAR offers a promising alternative to the 2D-RAKE with the early-late gate, offering an average increase in spectrum efficiency up to 100% in the presence of synchronization errors at both data rates of 9.6 and 128 Kbps.

In [1], we actually assessed the robustness of the multipath tracking module of STAR to various interesting design parameters such as sensitivity to the rolloff factor selection and the pulse-waveform errors of raised-cosine shaping filters. Here, we address another dimension that deserves investigation, *i.e.*, the robustness of the tracking module of STAR to possible power profile variations of Rayleigh fading. Indeed, a receiver is designed to operate satisfactorily in various radio-propagation conditions where the average

multipath powers can change “without notice”.

In [1], the significant performance gains of STAR have been demonstrated with equal-power paths. There it was shown that STAR can detect multipaths leaving deep fades above a detection threshold tuned to as low as -12 dB. Such extreme sensitivity to weak fade levels may suggest the need for a fine tuning of the tracking module and may raise concerns about lack of robustness to variations in propagation conditions. The question is whether STAR, tuned over equal-power paths, can cope with different multipath power profiles without significantly losing performance.

Link- and system-level simulation results suggest that profiles of (0, -3, -6) dB, (0, -6, -10) dB and (0, -6, -10) dB perform nearly as well as the (0, 0, 0) dB reference profile. The maximum capacity loss does not exceed 7% and suggest a strong robustness of STAR to variations in radio-propagation conditions. The 2D-RAKE exploits diversity less efficiently and hence its losses do not exceed 3%. Yet STAR maintains its performance advantage over the 2D-RAKE by about 50 to 60% in capacity for voice-rate links with low mobility.

II. DATA MODEL AND ASSUMPTIONS

We consider a single-user receiver structure on the uplink direction (portable-to-base station) of a cellular CDMA system. Let us assume that each base station is equipped with M receiving antennas. We consider P propagation paths in a selective fading multipath environment where the time-delay spread $\Delta\tau$ is small compared to T . The user binary phase shift keying bit sequence is first differentially encoded at a rate $1/T$, where T is the bit duration. The resulting sequence $b(t)$ is then spread with a binary pseudo-random noise sequence $c(t)$ at a rate $1/T_c$ where T_c is the chip pulse duration. For simplicity, the period of $c(t)$ is assumed to be equal to the bit duration T . The processing gain is given by $L = T/T_c$.

At successive frames of period T , we define the post-correlated observation vector by:

$$Z_n(t) = \frac{1}{T} \int_0^T X(nT + t + t')c(t')dt' . \quad (1)$$

where $X(t)$ is the observation vector received by the antenna array. After despreading the antenna-array signal vector, and framing the resulting post-correlation vector $Z(lT_c)$ over L chip samples at the bit rate:

$$\mathbf{Z}_n = [Z_n(0), Z_n(T_c), \dots, Z_n((L-1)T_c)] , \quad (2)$$

*: Work supported by the Bell/Nortel/NSERC Industrial Research Chair in Personal Communications and by the NSERC Research Grants Program.

we obtain the $M \times L$ post-correlation observation matrix \mathbf{Z}_n along the post-correlation model (PCM) as follows [2]:

$$\mathbf{Z}_n = \mathbf{H}_n s_n + \mathbf{N}_n = b_n \psi_n \mathbf{G}_n \mathbf{Y}_n \mathbf{D}_n^T + \mathbf{N}_n, \quad (3)$$

where $s_n = \psi_n b_n$ is the signal component, b_n is the transmitted DBPSK data sequence and ψ_n^2 is the total received power. $\mathbf{H}_n = \mathbf{G}_n \mathbf{Y}_n \mathbf{D}_n^T = \mathbf{J}_n \mathbf{D}_n^T$ with norm fixed to \sqrt{M} is the spatio-temporal propagation matrix, and $\mathbf{J}_n = \mathbf{G}_n \mathbf{Y}_n$ is the spatial response matrix which includes the effects of path loss, Rayleigh fading and shadowing. $\mathbf{G}_n = [G_{1,n}, \dots, G_{P,n}]$ is the $M \times P$ propagation matrix, and $\mathbf{Y}_n = \text{diag}[\varepsilon_{1,n}, \dots, \varepsilon_{P,n}]$ is the $P \times P$ diagonal matrix of normalized power ratios over multipaths $\varepsilon_{p,n}^2$ (*i.e.*, $\sum_{p=1}^P \varepsilon_{p,n}^2 = 1$). $\mathbf{D}_n = [D_{1,n}, \dots, D_{P,n}]$ is the $L \times P$ time-response matrix with columns:

$$D_{p,n} = [\rho_c(-\tau_{p,n}), \rho_c(T_c - \tau_{p,n}), \dots, \rho_c((L-1)T_c - \tau_{p,n})]^T$$

where $\{\tau_{p,n}\}_{p=1, \dots, P} \in [0, T)$ are the time-varying multipath-delays along the P paths and $\rho_c(t)$ is a truncated raised-cosine pulse which corresponds to the correlation function of a square-root raised-cosine shaping-pulse. \mathbf{N}_n is the $M \times L$ spatio-temporal uncorrelated noise matrix with variance σ_N^2 . It includes the thermal noise received at the antenna elements as well as the self-, in-cell and out-cell interference. We define the input SNR after despreading as $SNR_{\text{in}} = \psi^2 / \sigma_N^2$ and assume the time-variations of the channel to be very slow and locally constant relative to the bit duration T .

III. OVERVIEW OF THE 2D-RAKE AND STAR

We give brief overviews of the modified 2D-RAKE and enhanced STAR proposed in [1]. Evaluation of these two algorithms with different multipath power profiles will later confirm the performance advantage of STAR over the 2D-RAKE under different radio-propagation conditions.

A. Enhanced 2D-RAKE and the Early-Late Gate

First, assuming chip-oversampling at the rate $1/T_{sc}$ = k_s/T_c where $k_s > 1$ is an integer typically equal to 4, we compute the sample matrices $\hat{R}_{ZZ,n}^+(p)$ and $\hat{R}_{ZZ,n}^-(p)$ of $Z_{p,n}^+ = Z_n(\hat{\tau}_{p,n} + T_{sc})$ and $Z_{p,n}^- = Z_n(\hat{\tau}_{p,n} - T_{sc})$, respectively, for each tracked path. Secondly, we extract the corresponding pair of eigenvector-eigenvalue estimates $\{\hat{V}_n^+(p), \hat{\lambda}_n^+(p)\}$ and $\{\hat{V}_n^-(p), \hat{\lambda}_n^-(p)\}$, respectively. Finally, we update each multipath time-delay $\tau_{p,n}$ and the corresponding $M \times 1$ propagation vector $G_{p,n}$ for $p = 1, \dots, P_{\text{max}}$ (*i.e.*, maximum multipath fingers per antenna) by [1]:

$$a_{p,n} = \begin{cases} \text{Sign}\{\lambda_n^+(p) - \lambda_n^-(p)\} \\ \quad \text{if } |\lambda_n^+(p) - \lambda_n^-(p)| > \lambda_{\text{TH}}, \\ 0 \text{ otherwise,} \end{cases} \quad (4)$$

$$\hat{\tau}_{p,n+1} = \hat{\tau}_{p,n} + a_{p,n} T_{sc}, \quad (5)$$

$$\hat{G}_{p,n+1} = \begin{cases} \hat{V}_n^+(p) \text{ if } a_{p,n} = +1, \\ \hat{V}_n^-(p) \text{ if } a_{p,n} = -1, \\ \hat{V}_n^0(p) \text{ if } a_{p,n} = 0, \end{cases} \quad (6)$$

where λ_{TH} is the ‘‘clamping’’ threshold over the gap between the early-late eigenvalues below which the time-delay estimate is not incremented.

Neglecting the effect of synchronization errors, the despread vector-fingers $Z_{p,n} = Z_n(\hat{\tau}_{p,n})$ can be approximated at the estimated time-delays as:

$$Z_{p,n} \simeq G_{p,n} s_{p,n} + N_{p,n} = G_{p,n} \psi_n \varepsilon_{p,n} b_n + N_{p,n}. \quad (7)$$

Due to the fact that the propagation vector estimates suffer from phase ambiguities, differential demodulation is required and implemented as follows for DBPSK [4]:

$$\hat{s}_{p,n} = W_{p,n}^H Z_{p,n} = \hat{G}_{p,n}^H Z_{p,n} / M, \quad (8)$$

$$\hat{s}_n = \text{Real} \left\{ \sum_{p=1}^{P_{\text{max}}} \hat{s}_{p,n} \hat{s}_{p,n-1}^* \right\}, \quad (9)$$

$$\hat{b}_n = \text{Sign}\{\hat{s}_n\}. \quad (10)$$

B. Enhanced STAR

STAR replaces the two consecutive space and time combining steps of the 2D-RAKE by a joint step both in space and time. It transforms the matrix \mathbf{Z}_n into an ML -dimensional vector by arranging its columns in a single spatio-temporal column vector to obtain the following narrowband version of the PCM model [2]:

$$\mathbf{Z}_n = \mathbf{H}_n s_n + \mathbf{N}_n, \quad (11)$$

where \mathbf{H}_n and \mathbf{N}_n respectively denote the vector-reshaped matrices \mathbf{H}_n and \mathbf{N}_n in Eq. (3). Hence, it allows implementation of coherent space-time MRC combining as follows [2]:

$$\hat{s}_n = \text{Real}\{W_n^H \mathbf{Z}_n\} = \text{Real}\{\hat{\mathbf{H}}_n^H \mathbf{Z}_n / M\}. \quad (12)$$

Multipath synchronization (*i.e.*, both acquisition and tracking) is an implicit built-in step in the channel identification operation. It allows estimation of the number of multipaths \hat{P} , their time-delays $\hat{\tau}_{p,n}$ (*i.e.*, $\hat{\mathbf{D}}_n$), relative powers $\hat{\varepsilon}_{p,n}^2$ (*i.e.*, $\hat{\mathbf{Y}}_n$), and magnitudes and phases over all antennas in $\hat{\mathbf{G}}_n$. From these estimates, the channel identification unit reconstructs an accurate space-time channel vector estimate $\hat{\mathbf{H}}_n = \hat{\mathbf{G}}_n \hat{\mathbf{Y}}_n \hat{\mathbf{D}}_n^T$ [2].

The performance of the tracking module of STAR strongly depends on the accuracy, speed and stability of multipath detection of appearing and vanishing paths. The detection update rule adopted in this tracking module links the detection threshold δ_{TH}^2 defined as [1]:

$$\delta_{\text{TH}}^2 = \kappa \frac{\hat{\sigma}_{\text{res}}^2}{M} = \kappa \frac{\hat{\sigma}_N^2}{2M^2}, \quad (13)$$

to the residual noise estimate at the beamformer output:

$$\hat{\sigma}_{\text{res}}^2 = (1 - \alpha) \hat{\sigma}_{\text{res}}^2 + \alpha \left(\text{Imag} \left\{ \hat{\mathbf{H}}_n^H \mathbf{Z}_n / M \right\} \right)^2, \quad (14)$$

where α is a smoothing factor and $\hat{\sigma}_N^2 = 2M\sigma_{\text{res}}^2$ denotes an estimate of the input noise variance and κ a constant.

Vanishing Path: We decide that the p -th path has vanished at block iteration n_d if then and for a number of previous block iterations $n_v - 1$ its power $\hat{\psi}_n^2 \hat{\varepsilon}_{p,n}^2$ is constantly below δ_{TH}^2 , *i.e.*,

$$\hat{\psi}_n^2 \hat{\varepsilon}_{p,n}^2 < \delta_{\text{TH}}^2 \quad \text{for } n \in \{n_d - n_v + 1, \dots, n_d\}. \quad (15)$$

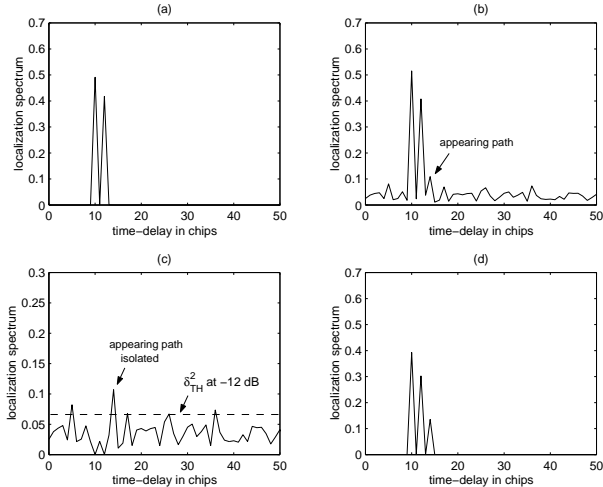


Fig. 1. Localization spectrum showing (a): the two paths being tracked using constrained channel estimate $\hat{\mathbf{H}}_n$ [2], (b): the two paths being tracked along with the appearing one using unconstrained channel estimate $\check{\mathbf{H}}_n$ [2], (c): the power of the appearing path being constantly detected above the threshold² δ_{TH}^2 using the residual channel $\delta\hat{\mathbf{H}}_n$, (d): the three paths being tracked using reconstructed $\hat{\mathbf{H}}_n$.

Appearing Path: The detection of an appearing path relies on a gross unconstrained channel estimate $\check{\mathbf{H}}_n$ [2]. It incorporates all multipath components including those newly appearing. From $\check{\mathbf{H}}_n$, we estimate the residual channel:

$$\delta\hat{\mathbf{H}}_n = \check{\mathbf{H}}_n \mathbf{\Pi}_{D_n}, \quad (16)$$

where the $L \times L$ projector¹ $\mathbf{\Pi}_{D_n}$ is given by:

$$\mathbf{\Pi}_{D_n} = \mathbf{I}_L - \hat{\mathbf{D}}_n \left(\hat{\mathbf{D}}_n^T \hat{\mathbf{D}}_n \right)^{-1} \hat{\mathbf{D}}_n^T, \quad (17)$$

and \mathbf{I}_L is $L \times L$ identity matrix. Then we base detection on the chip-sampled residual spectrum defined as:

$$\bar{S}_{\text{SS}}(kT_c) = \|\delta\hat{H}_{n,k}\|^2, \quad (18)$$

where $\delta\hat{H}_{n,k}$ is the k -th column of $\delta\hat{\mathbf{H}}_n$. At block iteration n_d , we decide that a new path has appeared at k -th chip (*i.e.*, $\hat{\tau}_{\hat{P}+1, n_d} = kT_c$) if, after a given number of block iterations n_a , $\bar{S}_{\text{SS}}(kT_c)$ consistently exceeds δ_{TH}^2 , *i.e.*,

$$\bar{S}_{\text{SS}}(kT_c) > \delta_{\text{TH}}^2 \quad \text{for } n \in \{n_d - n_a + 1, \dots, n_d\}. \quad (19)$$

In Fig. 1, we illustrate the detection process of an appearing path. We select the 9.6 Kbps voice-rate setup of section IV-A with $M = 4$ antennas and operate at $\text{SNR}_{\text{in}} \simeq -3$ dB after despreading.

In general, with 1, 2 or 4 antennas, tuning of κ in Eq. (13) to achieve best robustness and stability of synchronization led to a low path detection threshold δ_{TH}^2 ranging from -11 to -13 dB. Such extreme sensitivity to weak fade levels may suggest the need for a fine tuning of the tracking module and may raise concerns about lack of

¹Since $\hat{\mathbf{D}}_n^T \hat{\mathbf{D}}_n \simeq \mathbf{I}_{\hat{P}}$, inversion in Eq. (17) can be skipped.

²Other noise bursts are ignored. They may exceed the threshold, but only sporadically.

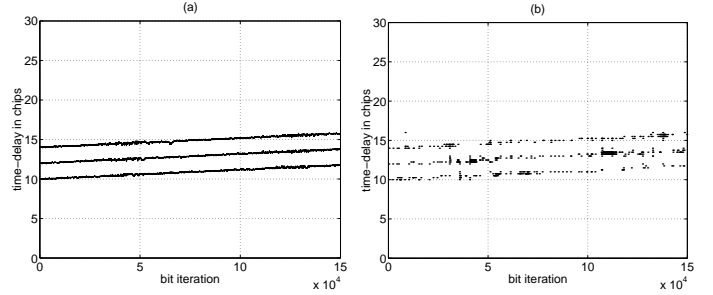


Fig. 2. Estimated time-delays $\hat{\tau}_{p,n}$ for a (0, 0, 0) dB multipath power profile. (a): STAR. (b): 2D-RAKE.

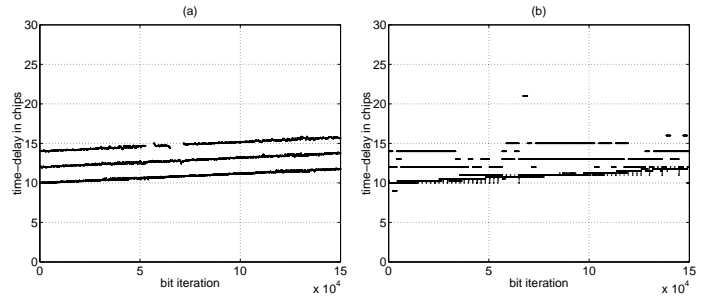


Fig. 3. Estimated time-delays $\hat{\tau}_{p,n}$ for a (0, -3, -6) dB multipath power profile. (a): STAR. (b): 2D-RAKE.

robustness to variations in propagation conditions. The question we address below is whether STAR, tuned over equal-power paths, can cope with different multipath power profiles without significantly losing performance.

IV. STUDY OF ROBUSTNESS TO MULTIPATH POWER PROFILE VARIATIONS

A. Simulation Setup

We consider a wideband CDMA system with 5 MHz bandwidth and $P = 3$ paths. The time-delays, ranked as 1st, 2nd and 3rd and initially set at $(10 T_c, 12 T_c, 14 T_c)$, vary linearly in time, with a drift of 0.046 ppm. The mobile has a speed of 1 Kmph corresponding to a Doppler shift of about 2 Hz at a carrier frequency of 2 GHz. The raised cosine roll-off is fixed to 0 (*i.e.*, truncated sinc). Power control (PC) requests an incremental change of ± 0.25 dB in transmitted power every 0.625 ms with a delay of 0.625 ms and an error of 10% over the PC bit command. The user information is encoded using a rate 1/2 convolutional code with constraint length $K = 9$. We consider a DBPSK voice rate of 9.6 Kbps with processing gain $L = 256$.

We use the capacity computation tool based on the work in [1] for evaluation of both STAR and the 2D-RAKE (or 1D-RAKE when $M = 1$) with $P_{\text{max}} = 5$, $k_s = 4$ and $n_{\text{RA}} = 1000$. n_{RA} denotes the 2D-RAKE reacquisition period in symbol iterations. Simulations are run for different multipath power profiles, *i.e.*, (0, -3, -6) dB, (0, -6, -10) dB and (0, -10, -10) dB. These profiles are chosen to be similar to those suggested by standards for performance validation [5]. We also assess both STAR and the 2D-RAKE in the reference situation of equal-power paths, *i.e.*, (0, 0, 0) dB.

B. Tracking Performance

Multipath detection update increases the stability of the tracking process, which in turn translates into a capacity gain. Figs. 2-a, 3-a, 4-a and 5-a illustrate the high level

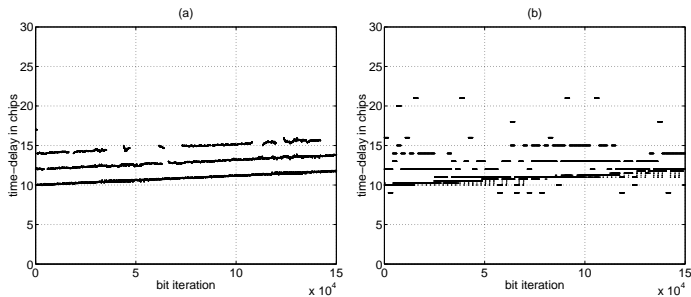


Fig. 4. Estimated time-delays $\hat{\tau}_{p,n}$ for a (0, -6, -10) dB multipath power profile. (a): STAR. (b): 2D-RAKE.

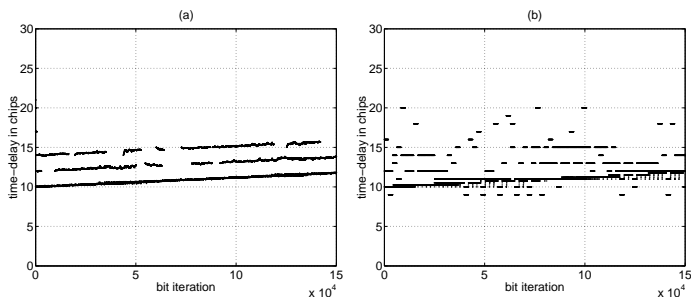


Fig. 5. Estimated time-delays $\hat{\tau}_{p,n}$ for a (0, -10, -10) dB multipath power profile. (a): STAR. (b): 2D-RAKE.

of stability and accuracy achieved by enhanced STAR during the tracking process in the four multipath power profile situations listed above, respectively. For comparison, Figs. 2-b, 3-b, 4-b and 5-b illustrate the tracking performance of the new combination of the 2D-RAKE [4] with the eigenvalue-based early-late gate proposed in [1]. It clearly shows more sensitivity, less stability and lower accuracy of the 2D-RAKE yet operating at about 1.5 dB higher in SNR than STAR. Indeed, the time-delay estimates are retrieved from the tracking modules of STAR and the 2D-RAKE, each operating at the corresponding SNR threshold that guarantees a maximum BER of 10^{-3} (see values in Tabs. 3 and 4).

As diversity decreases from the reference equal-power multipath situation nearly to the case of nonselective multipath [*i.e.*, (0, -10, -10) dB], tracking performance degrades, much more significantly with the 2D-RAKE than with STAR, however. The 2D-RAKE loses track of the useful paths and becomes relatively unstable, more so with paths that have weaker power. More frequent reacquisition is necessary to maintain “piece-wise” tracking of the multipath delays. On the other hand, STAR only sees a negligible increase in timing deviations while keeping much more solid track of the correct paths.

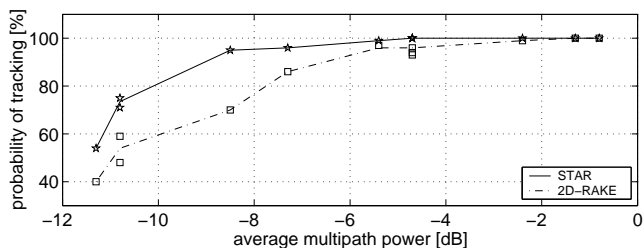


Fig. 6. Probability of tracking vs. the average multipath power for both STAR and the 2D-RAKE.

Multipath power profile [dB]	Probability of tracking [%]		
	1 st path	2 nd path	3 rd path
^(0,0,0) (-4.7, -4.7, -4.7)	100	100	100
^(0,-3,-6) (-2.4, -5.4, -8.5)	100	99	95
^(0,-6,-10) (-1.3, -7.3, -11.3)	100	96	54
^(0,-10,-10) (-0.8, -10.8, -10.8)	100	71	75

Tab. 1. Probability of multipath tracking of STAR for different multipath power profiles in 5MHz with 4 antennas and voice links @ 9.6 Kbps and BER = 10^{-3} .

Multipath power profile [dB]	Probability of tracking [%]		
	1 st path	2 nd path	3 rd path
^(0,0,0) (-4.7, -4.7, -4.7)	94	96	93
^(0,-3,-6) (-2.4, -5.4, -8.5)	99	97	70
^(0,-6,-10) (-1.3, -7.3, -11.3)	100	86	40
^(0,-10,-10) (-0.8, -10.8, -10.8)	100	59	48

Tab. 2. Probability of multipath tracking of the 2D-RAKE for different multipath power profiles in 5MHz with 4 antennas and voice links @ 9.6 Kbps and BER = 10^{-3} .

In Tabs. 1 and 2, we provide the *probability of tracking* for each path in each set of simulation (*i.e.*, with different multipath power profile) for both STAR and 2D-RAKE receiver. This probability is defined as the ratio of the time duration over which a given path is tracked by STAR over total simulation time. It should not be confused with the *probability of detection* of a path (*i.e.*, the probability of capturing a previously undetected path). As suggested in Figs. 2-b, 3-b, 4-b and 5-b, the *probability of tracking* is much more difficult to evaluate for the 2D-RAKE. Values reported in Tab. 2 are actually overoptimistic since we calculated the probability of tracking of the 2D-RAKE over the reacquisition instants only for simplicity. The tracking probability results for both STAR and the 2D-RAKE in Tabs. 1 and 2 (summarized in Fig. 6 vs. the average multipath power) suggest the following:

- STAR is able to maintain multipath tracking for almost a maximum duration of time, even for weak paths (see Tab. 1). For a path 3 dB weaker than the strongest path, tracking is barely lost, 1% of the time only. For a path 6 dB weaker than the strongest path, tracking is lost only about 4-5% of the time, regardless whether it is second or third in power. Even for a path as weak as 10 dB relative to the strongest path, tracking is lost only 46% of the time with the (0, -6, -10) dB profile. This is hardly surprising since its average power of -11.3 dB [*i.e.*, $0.1/(1+0.25+0.1)$] is only 0.7 dB above the detection threshold. With the (0, -10, -10) dB profile, however, its average power increases to -10.8 dB [*i.e.*, $0.1/(1+0.1+0.1)$] and hence tracking is lost only 25% of the time.

Multipath power profile	SNR [dB]	Capacity [users/cell]	Capacity loss [%]
(0,0,0)	-2.7	456	–
(0,-3,-6)	-2.7	442	3
(0,-6,-10)	-2.7	434	5
(0,-10,-10)	-2.7	425	7

Tab. 3. Link/system-level performance of STAR for different multipath power profiles in 5MHz with 4 antennas and voice links @ 9.6 Kbps and BER = 10^{-3} .

Multipath power profile	SNR [dB]	Capacity [users/cell]	Capacity loss [%]
(0,0,0) dB	-0.9	290	–
(0,-3,-6) dB	-1.1	287	1
(0,-6,-10) dB	-1.2	288	1
(0,-10,-10) dB	-1.2	280	3

Tab. 4. Link/system-level performance of the 2D-RAKE for different multipath power profiles in 5MHz with 4 antennas and voice links @ 9.6 Kbps and BER = 10^{-3} .

- The 2D-RAKE receiver is able to track a multipath about 100% of the time (see Tab. 2) only when its absolute average power is higher than -2 dB. With STAR, this threshold is around -5 dB. For an average multipath power below -8 dB, the probability of tracking readily drops to about 40% with the 2D-RAKE. With STAR, we reach the same loss figure only for an average power below -11.3 dB. STAR outperforms the 2D-RAKE in multipath tracking with different power profiles even though it operates at a required SNR about 1.5 dB lower than for the 2D-RAKE.

C. Link/System-Level Results

In Tabs. 3 and 4³, we provide link- and system-level performance results in terms of required SNR after despreading at a BER of 10^{-3} and in terms of capacity, respectively. These results suggest the following:

- In STAR, there is no impact of multipath power profile variations on the link-level performance in terms of required SNR (maintained at a constant value of -2.7 dB, see Tab. 3). A previous work arrived at a similar observation using diversity combining in IS-95 CDMA with perfect synchronization [6]. Indeed, given the high accuracy and probability of tracking of STAR, only a negligible amount of the maximum total power collectible in perfect synchronization is lost on average from undetected paths.

- In the 2D-RAKE, synchronization is not near-optimal like in STAR and hence variations in the multipath power profile have a noticeable impact on the required SNR. As the power profile approaches that of nonselective flat fading, the power of the first path becomes even more stronger thereby enabling a more stable synchronization at a required SNR 0.3 dB below the reference situation (see Tab. 4). With the 2D-RAKE, it is better to rely on a single path with stronger power than on multiple paths with weaker

³The new 2D-RAKE reference results reported here improve previous results in [1] by about 5% due to enhanced threshold tuning and increased stabilization of the early-late gate.

powers. These results are in agreement with previous observations [1] that the 2D-RAKE exploits diversity less efficiently than STAR.

- There is noticeable impact of multipath power profile variations on the system-level performance in terms of capacity in users per cell (see Tabs. 3 and 4). Best capacity is achieved in the strongest diversity condition with the equal-power profile. As the multipath power profile approaches that of a non-selective flat fading, diversity decreases, and so does capacity. The energy that is not captured from the undetected paths, although weak, spills over to interference in the system-level simulation and increases the variations of the incell and outcell interference as well as the outage probability [1], [6]. However, even though the impact of multipath power profile variations is noticeable at the system-level, capacity losses with the STAR are not significant and do not exceed 7%. The 2D-RAKE exploits diversity less efficiently and hence its losses, below 3%, are even less significant. Overall, under different radio-propagation conditions STAR maintains its performance advantage over the 2D-RAKE by about 50 to 60% in capacity for voice-rate links with low mobility.

V. CONCLUSIONS

In [1], STAR was shown to outperform the 2D-RAKE receiver. However, significant performance gains of STAR have been demonstrated with equal-power paths. There it was shown that STAR can detect multipaths leaving deep fades above a detection threshold tuned to as low as -12 dB. Such extreme sensitivity to weak fade levels may suggest the need for a fine tuning of the tracking module and may raise concerns about lack of robustness to variations in propagation conditions. By link- and system-level we demonstrate that STAR is indeed robust to multipath power profile variations. The maximum capacity loss does not exceed 7% with power profiles of (0, -3, -6), (0, -6, -10) and (0, -10, -10) dB. Therefore, no adaptive tuning is required to cope with varying propagation conditions. For voice-rate links with low mobility, STAR maintains its performance advantage over the 2D-RAKE by about 50 to 60% in capacity under different radio-propagation conditions.

REFERENCES

- [1] K. Cheikhrouhou, S. Affes, and P. Mermelstein, "Impact of synchronization on performance of enhanced array-receivers in wideband CDMA networks", *IEEE Journal on Selected Areas in Communications*, vol. 19, no. 12, pp. 2462-2476, December 2001.
- [2] S. Affes, P. Mermelstein, "A new receiver structure for asynchronous CDMA: STAR - the spatio-temporal array-receiver", *IEEE Journal on Selected Areas in Communications*, vol. 16, no. 8, pp. 1411-1422, October 1998.
- [3] R. Prasad and T. Ojanperä, "An overview of CDMA evolution toward wideband CDMA", *IEEE Communications Surveys*, vol. 1, no. 1, Fourth Quarter 1998.
- [4] A.F. Naguib, *Adaptive Antennas for CDMA Wireless Networks*, Ph.D. dissertation, Stanford University, Stanford, CA, 1996.
- [5] 3rd Generation Partnership Project, Technical Specification Group Radio Access Networks, *UTRA (BS) FDD; Radio Transmission and Reception*, 3GPP TS 25.104, V4.1.0, 2001.
- [6] A. Jalali and P. Mermelstein, "Effects of diversity, power control, and bandwidth on the capacity of microcellular CDMA systems", *IEEE Journal on Selected Areas in Communications*, vol. 12, no. 5, pp. 952-961, June 1994.